Use of Narrow-Band Spectra to Estimate the Fraction of Absorbed Photosynthetically Active Radiation

Forrest G. Hall and Karl F. Huemmrich

NASA Goddard Space Flight Center, Greenbelt, Maryland

Samuel N. Goward

Remote Sensing Systems Laboratory and Department of Geography, University of Maryland

We propose a novel approach for using high-spectral resolution imagers to estimate the fraction of photosynthetically active radiation adsorbed, f_{apar}, by vegetated land surfaces. In comparison to approaches using broad-band vegetation indices, the proposed method appears to be relatively insensitive to the reflectance of nonphotosynthetically active material beneath the canopy, such as leaf litter or soil. The method is based on a relationship between the second derivative of the reflectance vs wavelength function for terrestrial vegetation and f_{apar}. The relationship can be defined by the second derivatives in either of two windows, one in the visible region centered at 0.69 μm, another in the near-infrared region centered at 0.74 μm.

INTRODUCTION

The fraction of incident photosynthetically active radiation absorbed, f_{apar}, by vegetated land surfaces is an important variable in understanding the energy budget and hydrology at the land–atmo-

sphere interface (Sellers et al., 1986). For example, under fixed atmospheric evaporative demand, the evaporation rate from a well-watered, vegetated soil is directly proportional to f_{apar} (Monteith, 1973). Seasonally accumulated f_{apar} is also an important variable in determining net primary production, dry-matter production, and crop grain yields (Monteith, 1977; Goward et al., 1985; Daughtry et al., 1983).

Many previous studies have investigated relationships between remotely sensed reflectance and f_{apar} [for example, see Hatfield et al. (1984), Asrar et al. (1985; 1986), Choudhury (1987), and Sellers (1987a,b)]. These studies however, have focused on the contrast in the broad-band (≥ 0.1 μm in width) visible and near-infrared reflectance between the canopy photosynthetic elements and the nonphotosynthetic background or soil. Although these studies have demonstrated various relationships between f_{apar} and spectral-reflectance indices, Choudhury (1987) has found that the relationships can be very sensitive to variations in the reflectance of the nonphotosynthetic background (e.g., leaf litter or soil).

In this paper, we develop an approach for the estimation of f_{apar} using the second derivative of the spectral reflectance function with respect to

wavelength, $\rho''(\lambda)$, and show two narrow windows within the domain 0.5–0.9 μm, where $\rho''(\lambda)$ is a monotonic increasing function of f_{apar}, independent of the soil or nonphotosynthetic background. This phenomena occurs primarily because the slope of the background reflectance is changing very slowly with wavelength, whereas the slope of the reflectance of photosynthetic canopy elements is changing more rapidly. This theoretical investigation suggests the utility of a narrow-band (~ 0.03–0.01 μm) sensor with a minimum of three bands (necessary to calculating the second derivative) located in selected spectral windows for estimating f_{apar}.

THEORETICAL DEVELOPMENT

A simple argument relating $\rho''(\lambda)$ and f_{apar} can be developed as follows. For a collection of opaque, photosynthetic canopy elements with reflectance $\rho_c(\lambda)$, distributed on nonphotosynthetic elements (soil, leaf litter, or snow) with reflectance $\rho_b(\lambda)$, the reflectance $\rho(\lambda)$ of the canopy/background combination is given by

$$\rho(\lambda) = \alpha\rho_c(\lambda) + (1 - \alpha)\rho_b(\lambda), \qquad (1)$$

where α is the likelihood of viewing a photosynthetic canopy element from the sensor and $(1 - \alpha)$ the likelihood of viewing a background element. Equation (1) represents a highly oversimplified treatment but is helpful in understanding the basis of the relationship between f_{apar} and $\rho''(\lambda)$. We will substitute a more rigorous treatment shortly to examine the validity of the concept.

The second derivative of Eq. (1) is given by

$$\rho''(\lambda) = \alpha\rho_c''(\lambda) + (1 - \alpha)\rho_b''(\lambda). \qquad (2)$$

Now, for spectral regions where the slope of $\rho_c''(\lambda)$ $\gg \rho_b''(\lambda)$, it is clear from Eq. (2) that

$$\rho''(\lambda) = \alpha\rho_c''(\lambda) \qquad (3)$$

or

$$\alpha = \rho''(\lambda)/\rho_c''(\lambda). \qquad (4)$$

From Figure 1a), which shows $\rho_b(\lambda)$ for a variety of soils (Stoner and Baumgardner, 1981) and leaf litter (Hall et al., 1990), it is clear that there are many spectral regions where the slope of $\rho_b(\lambda)$ is changing very slowly or not at all. Figure 1b) shows $\rho_c(\lambda)$ for a red maple leaf (Brakke, 1989). There are a number of regions where the condition $\rho_c''(\lambda) \gg \rho_b''(\lambda)$ should hold and α should be

independent of the background reflectance. Such a technique is well known in analytical chemistry for detecting specific chemical elements within a complex background of other chemical compounds (O'Havers, 1982; Butler and Hopkins, 1970; Talsky et al., 1978). Demetriades-Shah and Steven (1988) have used this approach to detect leaf chlorosis in sugar beet canopies.

It is also true in this simple model of canopy reflectance that the likelihood of viewing a canopy element can be modeled as

$$\alpha = 1 - e^{-kL}, \qquad (5)$$

where L is the leaf area index and k is the canopy attenuation coefficient. A number of researchers, for example, Monteith (1973) or Norman (1975), have suggested that f_{apar} can be estimated by

$$f_{apar} = 1 - e^{-k'L}. \qquad (6)$$

Combining Eqs. (4), (5), and (6), f_{apar} can be expressed in terms of the second derivatives as

$$f_{apar} = 1 - e^{-k'/k\ln(\alpha - 1)}. \qquad (7)$$

If $k' \sim k$ then

$$f_{apar} \approx \alpha = \rho''(\lambda)/\rho_c''(\lambda), \qquad (8)$$

which suggests a linear relationship between f_{apar} and $\rho''(\lambda)$ independent of the background reflectance and depends only upon the second derivative of the total canopy/background reflectance and the reflectance of the photosynthetic material of the canopy itself.

Although this expression has humble beginnings mathematically, it led us to try a more rigorous approach to see if the basic idea held up.

NUMERICAL SIMULATION

We used the SAIL (Scattering from Arbitrarily Inclined Leaves) canopy reflectance model (Alexander, 1983; Verhoef, 1984) to generate $\rho(\lambda)$ at 0.01 μm intervals between 0.5 μm, and 0.9 μm. The SAIL model calculates bidirectional reflectances for a canopy consisting of horizontally uniform layers. A single layer containing only leaves with a spherical leaf angle distribution was used in this model. Canopy reflectances were calculated for nadir viewing angles using 10 different LAI values (0.01, 0.25, 0.50, 0.75, 1, 2, 3, 4, 5, 7) each with a variety of soil backgrounds. Leaf re-
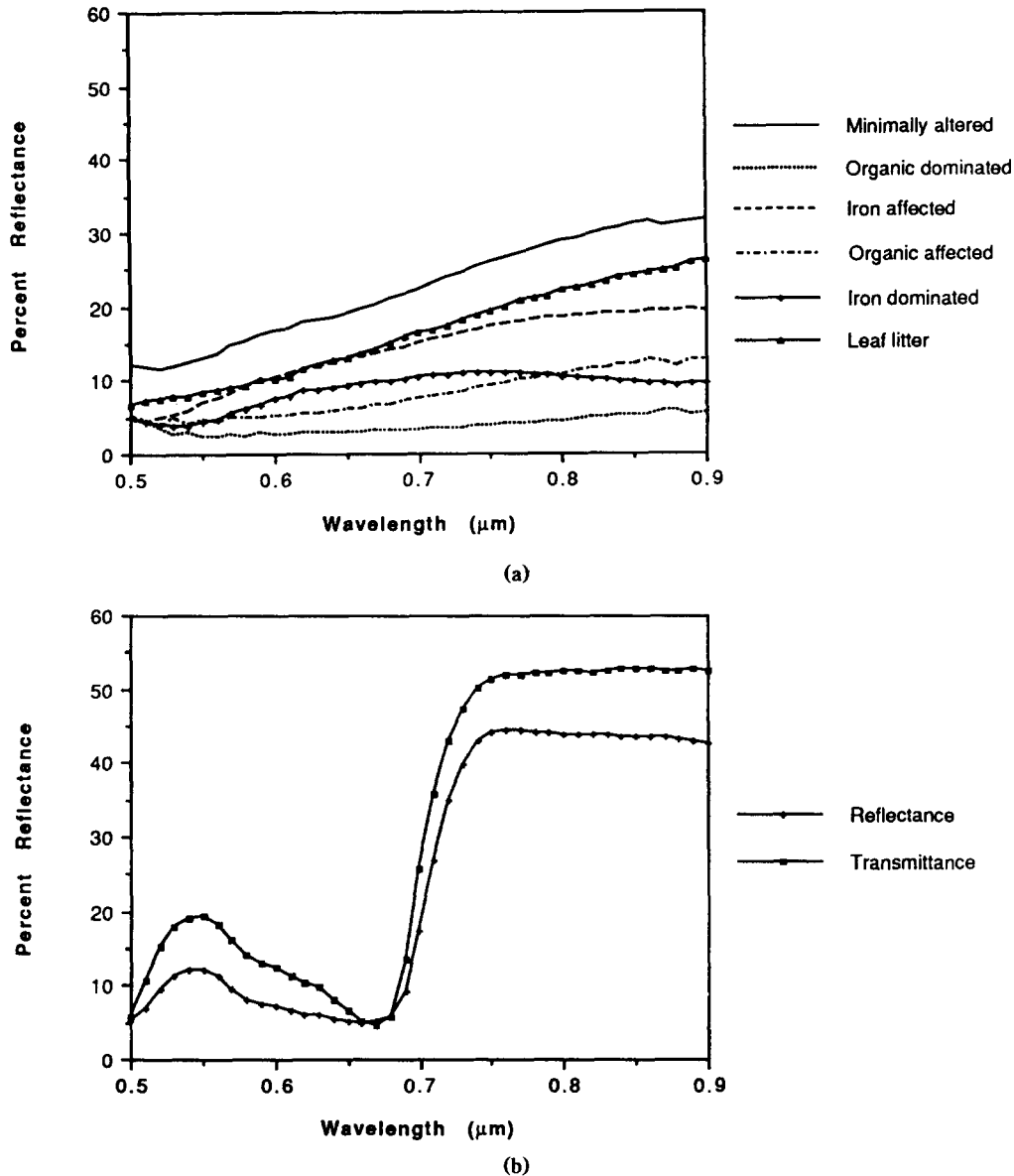
Figure 1. a). Background reflectances; leaf litter reflectances from Hall et al. (1990); other soil reflectances from Stoner et al. (1980). b). Leaf optical properties; data averaged from red maple leaf optical properties collected by Brakke (1989) using a SE-590 spectrometer.

flectance and transmittance values came from measurements of a red maple (*Acer rubrum*) leaf using a Spectron Engineering SE-590 spectrometer (Brakke, 1989). The SE-590 data were averaged to 0.01 μm bands [Fig. 1b)]. The model runs simulate a clear day, 10:00 a.m. local time at the vernal equinox and 40°N latitude.

Stoner and Baumgardner (1981) describe five distinct types of soil reflectance functions: organic dominated, minimally altered, iron affected, organic affected, and iron dominated. Examples of each of these types of soil (Stoner et al., 1980)

were used as background in the model. Leaf litter reflectance functions measured with the Cary-14 radiometer were also included as background in the study (Hall et al., 1990). Figure 1a) shows all of the background reflectance functions used.

Figures 2a) and b) are families of $\rho(\lambda)$ functions generated from the SAIL model for two of the soil backgrounds. Each line corresponds to $\rho(\lambda)$ for a specific LAI value. Notice the differences in reflectance values in the visible bands (around 0.65–0.69 μm) and near infrared bands (above 0.74 μm) due to the different reflectances
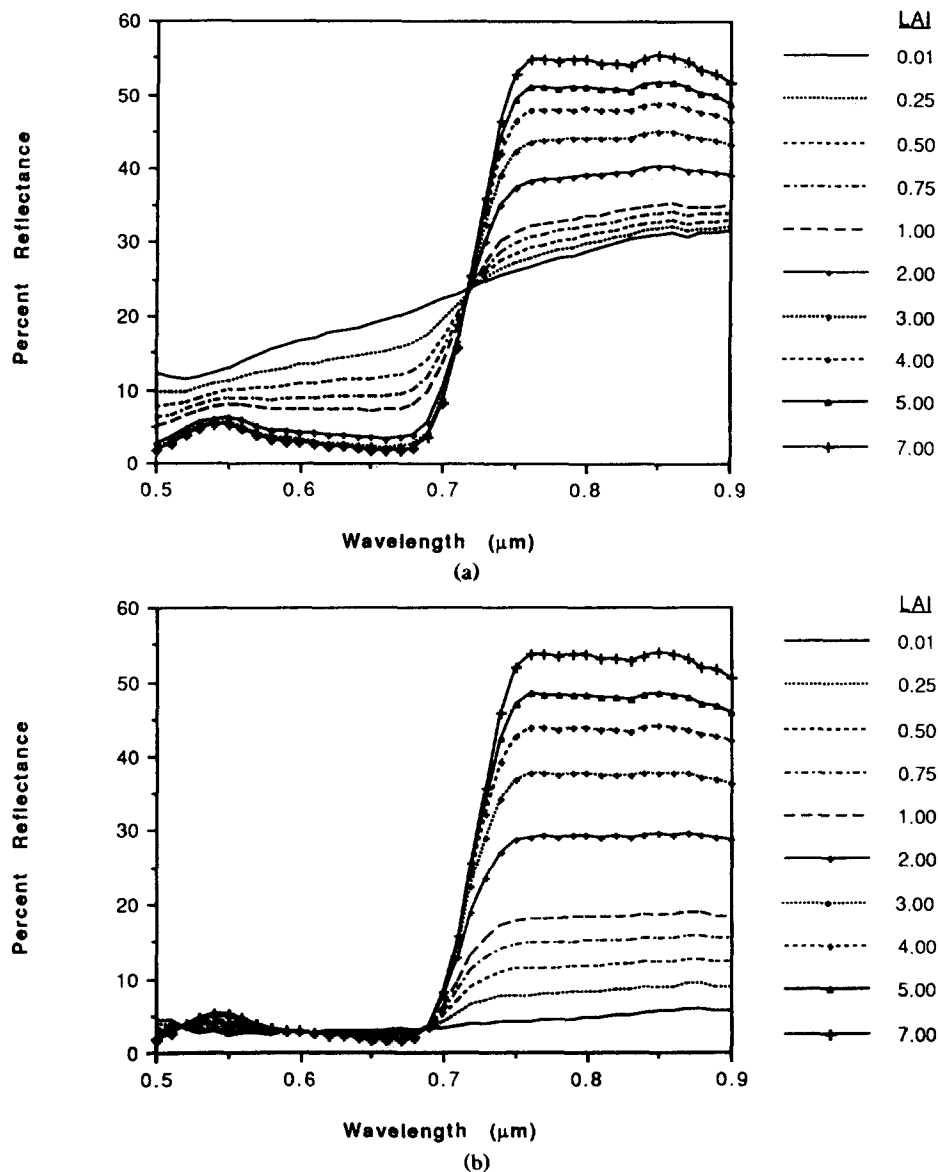
Figure 2. Canopy reflectance families calculated from SAIL model for a red maple canopy over differing soil backgrounds: a) minimally altered soil; b) organic dominated soil. Each function is for a different value of LAI. The function which has the lowest reflectance at 0.9 μm is associated with an LAI of 0.01 and increases sequentially corresponding to LAI values of 0.25, 0.50, 0.75, 1, 2, 3, 4, 5, and 7.

of the background for canopies with the same LAI. For example, at 0.68 μm the canopy with a LAI of 1 and minimally altered soil background has a reflectance of 7.75%, whereas the same canopy with organic dominated soil background has a reflectance of 2.29%. In the near infrared at 0.78 μm canopies with LAI of 1 have reflectances of 32.89% and 17.98% for minimally altered and organic dominated soil backgrounds, respectively. Variations in the red and near infrared reflectances resulting from variations in background optical

properties cause variability in the traditional vegetation indices, such as simple ratio or normalized difference vegetation index (Huete et al., 1985).

For each of the $\rho(\lambda)$ functions generated from the SAIL model the second derivative $\rho''(\lambda)$ is estimated numerically at each wavelength λ_i using

$$\rho''(\lambda_i) = \{\rho(\lambda_{i+1}) - 2\rho(\lambda_i) + \rho(\lambda_{i-1})\}/\Delta\lambda^2.$$

$$(10)$$

Gans (1982) discusses and provides solutions to

some of the problems associated with measurement noise in the calculation of $\rho''(\lambda_i)$. The second derivative is very sensitive to noise. This simple calculation of the second derivative is possible in this study because the model produces idealized spectral reflectances which have little noise. Actual spectral reflectance measurements will require some smoothing. The second derivatives for the $\rho(\lambda)$ functions shown in Figures 2a) and b) are plotted in Figures 3a) and b). $\rho_b(\lambda)$ has the greatest effect on $\rho''(\lambda)$ in the wavelengths between 0.50 μm and 0.60 μm. As seen in Figure 1a) this is the region of greatest change in slope

for the soil reflectance functions. Two optimum windows occur where $\rho_c''(\lambda) \gg \rho_b''(\lambda)$. These windows are centered at 0.69 μm and 0.74 μm, as seen in Figure 2. The optimum regions are found at the reflectance minimum caused by chlorophyll absorption and at the knee of the near-infrared plateau.

We also used the SAIL model to determine daily f_{apar}, the ratio of the energy absorbed by the canopy over the day, and the total incoming energy in the visible wavelengths between 0.5 μm and 0.7 μm. In order to calculate a bidirectional reflectance, the SAIL model first determines the

Figure 3. Second derivatives of canopy reflectance functions. Line types in each plot corresponds to line types used in reflectance plots (Fig. 2). Background reflectances: a) minimally altered soil; b) organic dominated soil.

Wavelength (μm)

(a)

Wavelength (μm)

(b)
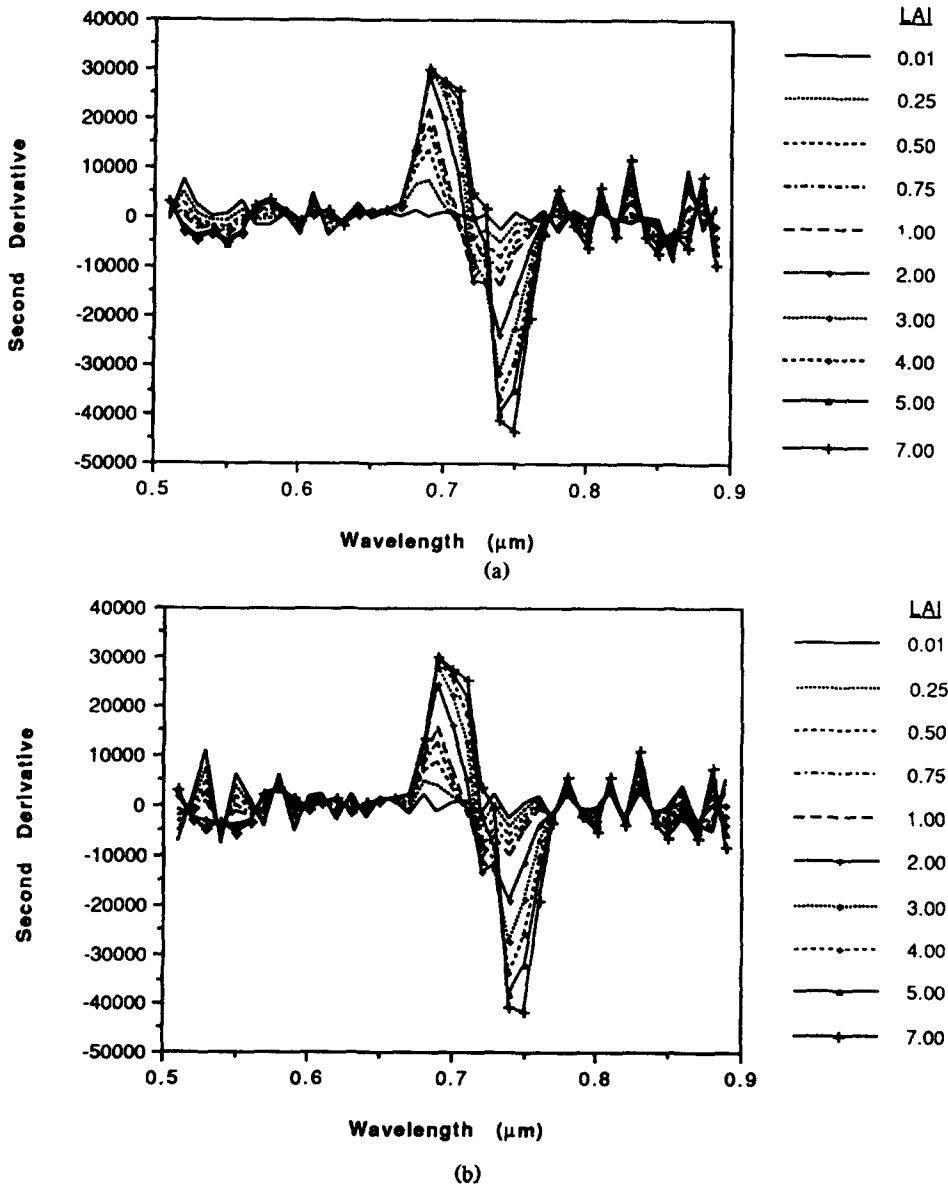
direct beam and the upward and downward diffuse flux densities at all levels in the canopy. These flux values are used to calculate the amount of energy absorbed by the canopy by finding the difference between energy entering and leaving the canopy. The absorbed energy values are integrated throughout the daylight period for the wavelengths between 0.5 μm and 0.7 μm. The daily absorbed energy is compared to the incoming energy to determine f_{apar} (Goward and Huemmrich, 1990).

The second derivatives at the two optimum windows, centered on 0.69 μm and 0.74 μm, are plotted against f_{apar} in Figures 4a) and 4b). For comparison the effects of the background on the normalized difference vegetation index (NDVI) and f_{apar} can be seen in Figure 5. As suggested from Eq. (8), sensitivity to background reflectance of the relationship between $\rho''(\lambda)$ and f_{apar} is minimized. At 0.69 μm the assumption of opaque leaves is nearly satisfied [see Fig. 1b)] and the relationship is approximately linear. At 0.74 μm

Figure 4. Percent daily absorbed photosynthetically active radiation ($f_{apar} * 100$) versus the second derivatives of the canopy reflectance functions. Each line is for the different background types: a) second derivative at 0.69 μm; b) second derivative at 0.74 μm.
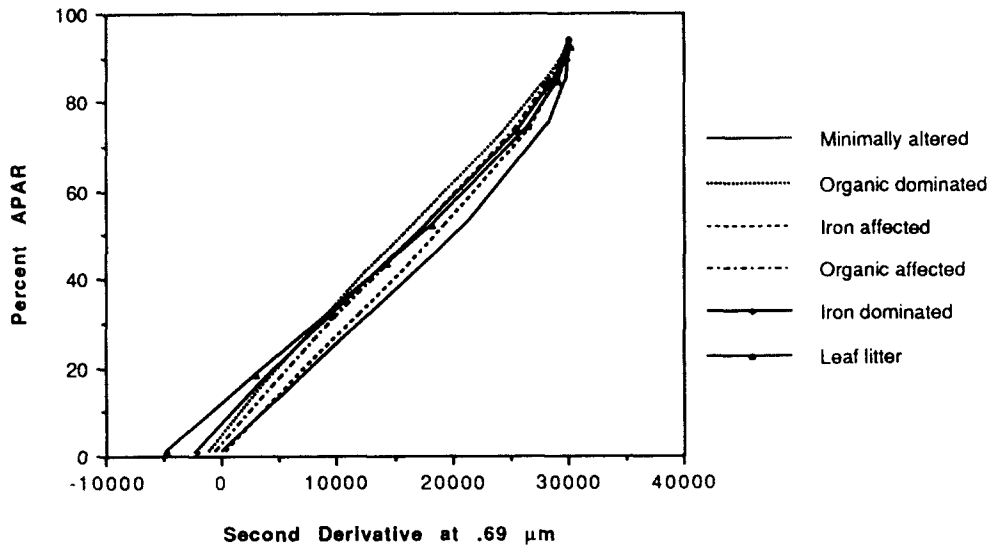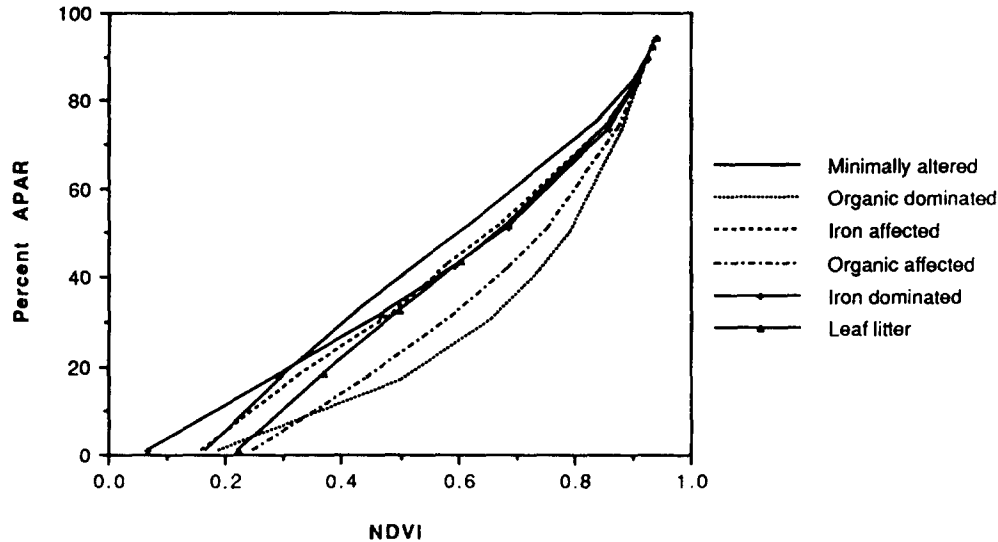

(a)
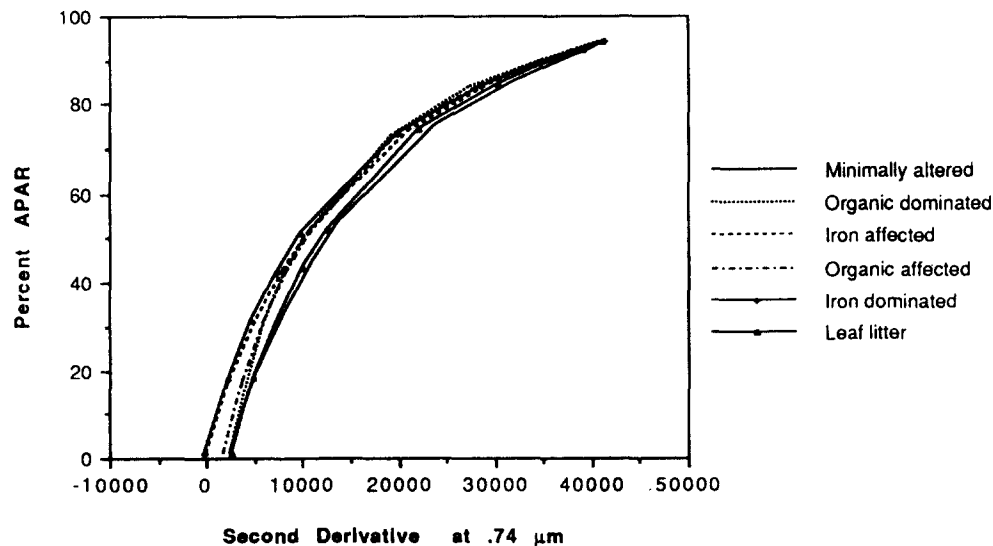
(b)

Figure 5. Percent daily absorbed photosynthetically active radiation ($f_{apar} * 100$) versus the normalized difference vegetation index (NDVI), where NDVI is given by NDVI = $[\rho(0.77 \mu m) - \rho(0.66 \mu m)]/[\rho(0.77 \mu m) + \rho(0.66 \mu m)]$. Each line is for the different background types.

the leaves are more translucent; thus, the relationship between $\rho''(\lambda)$ and f_{apar} is nonlinear, but remains relatively insensitive to background reflectance.

CONCLUSION

A simple conceptual model and numerical simulation show that the $\rho''(\lambda)$ is related to f_{apar}. By choosing spectral regions where $\rho_c''(\lambda)$ is large and $\rho_b''(\lambda)$ is small, the effects of the nonphotosynthetic canopy and background elements on the relationship between $\rho''(\lambda)$ and f_{apar} may be minimized.

A number of existing or planned remote sensing instruments possess narrow bands (0.01 μm or less) in the optimum windows defined by our analysis. A minimum of three narrow-wavelength bands within the window would be required to determine the second derivative. The second derivative is very sensitive to noise; therefore, it is very important to have precise calibration of the detector for each band. To minimize the effects of noise in the spectral reflectance data, more wavelength bands could be introduced to allow for smoothing of the data.

We are in the process of evaluating this approach using narrow-band spectrometer data collected concurrently with absorbed, photosynthetically active radiation data from a grassland prairie

during FIFE, Sellers and Hall (1989). This evaluation will be the basis for a future paper.

REFERENCES

Alexander, L. (1983), SAIL Canopy Model Fortran Software, NASA Contract No. NAS 9-15800.

Asrar, G., Fuchs, M., Kanemasu, E. T., and Hatfield, J. L. (1985), Estimating absorbed photosynthetic radiation and leaf area index from spectral reflectance measurements in wheat, *Agron. J.* 76:300–306.

Asrar, G., Kanemasu, E. T., Miller, G. P., and Weiser, R. L. (1986), Light interception and leaf area estimates from measurements of grass canopy reflectance, *IEEE Trans. Geosci. Remote Sens.* GE-24(1):76–82.

Brakke, T. (1989), Goddard Space Flight Center, Code 923, personal communication.

Butler, W. L., and Hopkins, D. W. (1970), Higher derivatives analysis of complex absorption spectra, *Photochem. Photobiol.* 12:439–450.

Choudhury, B. J. (1987), Relationships between vegetation indices, radiation absorption and net photosynthesis evaluated by a sensitivity analysis, *Remote Sens. Environ.* 22:209–234.

Daughtry, C. S. T., Gallo, K. P., and Bauer, M. E. (1983), Spectral Estimates of solar radiation intercepted by corn canopies, *Agron. J.* 75:527–731.

Demetriades-Shah, T. H., and Steven, M. D. (1988), High spectral resolution indices for monitoring crop growth and chlorosis, in *Proceedings of the 4th Int. Colloq. on Spectral*

Signatures of Objects in Remote Sensing, ESA SP-287, April 1988, pp. 299–302.

Gans, P. (1982), Derivative spectroscopy and its applications in analysis: numerical methods for generating derivative spectra, *Anal. Proc.* (Jan.):33–35.

Goward, S. N., and Huemmrich, K. F. (1990), Remote sensing of the absorption of photosythetically active radiation by vegetation canopies: an assessment using the SAIL model, forthcoming.

Goward, S. N., Tucker, C. J., and Dye, D. G. (1985), North American vegetation patterns observed with the Nimbus-7 Advanced Very High Resolution Radiometer, *Vegetatio* 64:3–14.

Hall, F. G., Huemmrich, K. F., Strebel, D. E., Goetz, S. J., Nickeson, J. E., and Woods, K. (1990), Biophysical, morphological, canopy optical property, and productivity data from The Superior National Forest, Goddard Space Flight Center, Code 923, Greenbelt, MD.

Hatfield, J. L., Asrar, G., and Kanemasu, E. T. (1984), Intercepted photosynthetically active radiation estimated by spectral reflectance, *Remote Sens. Environ.* 14:65–75.

Huete, A. R., Jackson, R. D., and Post, D. F. (1985), Spectral response of a plant canopy with different soil backgrounds, *Remote Sens. Environ.* 17:37–53.

Monteith, J. L. (1973), *Principles of Environmental Physics.* Edward Arnold, London.

Monteith, J. L. (1977), Climate and the efficiency of crop production in Britain, *Phil. Trans. Roy. Soc. Lond.* B281:277–294.

Norman, J. M. (1975), Radiative transfer in vegetation, in *Heat and Mass Transfer in the Biosphere. I. Transfer Processes in Plant Environment* (D. A. deVries and N. H. Afgan, Eds.), Wiley, New York.

O'Havers, T. C. (1982), Derivative spectroscopy and its applications in analysis: derivative spectroscopy: theoretical aspects. Plenary Lecture, *Anal. Proc.* (Jan.):22–28.

Sellers, P. J. (1987a), Relations between canopy reflectance, photosynthesis and transpiration: links between optics, biophysics and canopy architecture, *Adv. Space Res.* 7(11):27–44.

Sellers, P. J. (1987b), Canopy reflectance, photosynthesis, and transpiration. II. The role of biophysics in the linearity of their interdependence, *Remote Sens. Environ.* 21:143–183.

Sellers, P. J., and Hall, F. G. (1989) (Eds.), FIFE-89 Experimental Plan, NASA Goddard Space Flight Center, Code 923, Greenbelt, MD.

Sellers, P. J., Mintz, Y., Sud, Y. C., and Dalcher, A. (1986), A simple biosphere model (SiB) for use within general circulation models, *J. Atmos. Sci.* 43:505–531.

Stoner, E. R., and Baumgardner, M. F. (1981), Characteristic variations in reflectance of surface soils, *Soil Sci. Soc. Am. J.* 45(6):1161–1165.

Stoner, E. R., Baumgardner, M. F., Biehl, L. L., and Robinson, B. F. (1980), Atlas of soil reflectance properties, Agric. Exp. Stn. Res. Bull. No. 962. Purdue Univ., West Lafayette, IN.

Talsky, G., Mayring, L., and Kreuzer, H. (1978), High-resolution, higher-order UV/VIS derivative spectrophotometry, *Angew. Chem. Int. Ed. Engl.* 17:785–799.

Verhoef, W. (1984), Light scattering by leaf layers with application to canopy reflectance modeling: the SAIL model, *Remote Sens. Environ.* 16:125–141.